Annals of Phytomedicine 14(2): 668-679, 2025

DOI: http://dx.doi.org/10.54085/ap.2025.14.2.67

Annals of Phytomedicine: An International Journal
http://www.ukaazpublications.com/publications/index.php

Print ISSN : 2278-9839 Online ISSN : 2393-9885

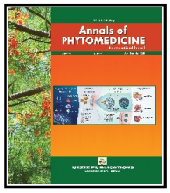

Original Article : Open Access

Analysis of physicochemical characteristic and antifungal potential of silver nanoparticles against Alternaria blight pathogenesis in *Brassica juncea*

Sandhya Upadhyay*, Anjali Sharma*, S. K. Najrul Islam, Absar Ahmad** and Gohar Taj*◆**

** Department of Molecular Biology and Genetic Engineering, College of Basic Sciences and Humanities, GBPUA&T, Pantnagar-263145, Uttarakhand, India*

*** Interdisciplinary Nanotechnology Centre (INC), AMU, Aligarh-202002, Uttar Pradesh, India*

Article Info

Article history
Received 22 September 2025
Revised 25 October 2025
Accepted 26 October 2025
Published Online 30 December 2025

Keywords
Alternaria
Antifungal
Brassica
Nanoparticles
Silver and
spectroscopy

Abstract

Silver nanoparticles represent a sustainable and environmentally friendly alternative to conventional antimicrobial agents, offering a potent strategy for phytodisease management without raising ethical issues and intoxication to environmental and human health. This study evaluates the physicochemical characteristics and antifungal effectiveness of silver nanoparticles (Ag_2O and Ag) against *Alternaria brassicae*, the causative agent of Alternaria blight disease. Nanoparticles were characterized by means of various techniques, including DLS, FTIR, TEM and UV-Visible spectroscopy, confirming their successful synthesis, average sizes, particle distribution, morphology and associated capping agents. Antifungal activity was determined through the poisoned food method, disease severity index and cytomorphological variations using light and scanning electron microscopy. Both nanoparticles significantly disintegrated fungal mycelia and reduced conidia germination at 80 ppm *in vitro* while effectively decreasing the number and size of blight lesions in *Brassica juncea* under *in vivo* conditions, thereby revealing the antifungal efficacy of silver nanoparticles.

1. Introduction

Cruciferous oilseeds are essential crops, serving as concentrated sources of energy that play a vital role in human diets. Among the Brassicaceae family, *B. juncea* stands out as one of the prominent cultivated crops because of its high oil content, covering essential fatty acids, fat-soluble vitamins, protein and antioxidants (Sharma *et al*., 2017). It is grown across tropical and subtropical regions, accounting for 28.6% of global production. Beyond its edible oil, it can be utilized in multiple ways such as leafy vegetables, oilseed meal cakes for animal feed, green manure, biodiesel and as a functional bio-fumigant to manage pests and pathogens (Meena *et al*., 2012). Moreover, its nutraceutical and pharmacological properties hold significant medicinal value, contributing to the prevention of several non-communicable diseases (Abdallah *et al*., 2020). However, after cultivating over 26.2 million hectares, India reliant on imports to meet domestic demand (Thakur *et al*., 2020) because the crop faces significant challenges in achieving optimal harvest indices and oil content, primarily due to certain biotic stress, specially fungus due to its susceptible nature towards disease like Sclerotinia stem rot, Alternaria blight and White rust (Verma *et al*., 2023).

Alternaria is a ubiquitous genus of microfungi comprising saprophytic, endophytic, and pathogenic species and it is responsible for a destructive phytodisease known as Alternaria blight or black spot caused by *A. brassicae*. This necrotrophic fungus poses a serious threat to almost all members of the cruciferous family, leading to yield losses of up to 70% (Regar *et al*., 2024). The pathogen impairs photosynthetic efficiency and induces premature ripening of seeds, resulting in marked decline in seed quality and oil content. In addition to its phytopathogenicity, Alternaria produces airborne spores that act as allergens, contributing to hypersensitivity reactions and asthma in humans (Kumar *et al*., 2016). To mitigate the effects of Alternaria blight, different kinds of synthetic fungicides have been extensively applied. However, these chemicals pose considerable health issues and environmental risks. For example, mancozeb has been linked to hepatotoxicity, epidermal necrolysis and impaired fertility in humans and certain animals (Pirozzi *et al*., 2016), while carbendazim has confirmed genotoxicity and hematological alterations (Hashim *et al*., 2023). Furthermore, the excessive use of such fungicides alters soil texture and disrupts microbial communities, thereby affecting soil health and sustainability.

Nanotechnology offers a promising avenue to revolutionize agriculture and food systems through its diverse applications in disease management, early pathogen detection, pest control, food packaging and nano-fertilizers (Kale *et al*., 2021). Moreover, nanoparticles (NPs) are a sustainable, cost-effective and eco-friendly alternative to conventional fungicides. Generally, nanometals like silver, gold, zinc and copper are highly effective in dropping microbial growth due to their biostatic and biocidal properties. Among them, silver NPs have remarkable physicochemical properties and broad-spectrum antimicrobial activity. It is known to rupture microbial membranes by inducing reactive oxidative burst and hindering cellular pathways (Ficerman *et al*., 2022). Despite their promising potential,

Corresponding author: Dr. Gohar Taj
Professor, Department of Molecular Biology and Genetic Engineering, College of Basic Sciences and Humanities, GBPUA&T, Pantnagar-263145, Uttarakhand, India
E-mail:gohartajkhan@rediffmail.com
Tel.: +91-7906553007

further research should be required to fully understand the antimicrobial effects of NPs and the key factors influencing their activity, including concentration, exposure duration, particle morphology, size and the specific form of silver NPs.

2. Materials and Methods

2.1 Collection of nanoparticles, plant material and pathogen

The studied silver NPs [oxide (Ag_2O) and elemental (Ag)] were obtained from the Interdisciplinary Nanotechnology Centre, Aligarh Muslim University. The seeds of *B. juncea* var. Varuna were collected from the Department of Plant Breeding and Genetics, College of Agriculture. Spores of *A. brassicae* were recovered from Brassica plants exhibiting Alternaria blight symptoms from the Crop Research Centre (CRC) at Govind Ballabh Pant University of Agriculture and Technology by using the single-cell isolation onto V8 juice agar medium (Strandberg, 1987; Zhang *et al*., 2013). The identity of *A. brassicae* was verified by examining its morphological features, such as colony colour, texture, conidial size and structure, as well as by pathogenicity test on leaves of *B. juncea*, which satisfied Koch's postulates (Bhunjun *et al*., 2021).

2.2 Physiochemical characterization of silver nanoparticles

The quality of both Ag_2O and Ag NPs was analyzed using UV-Vis spectroscopy (Biospectrometer, Eppendorf) within a wavelength range of 250 to 600 nm, with deionized water as the blank. The surface morphology and average particle size distribution were determined by TEM and DLS (Malvern, Panalytical), respectively. The presence of reducing agents and functional groups on the surface of silver NPs was analysed by FT-IR spectrometer (Alpha II, Bruker) and illustrated through the peaks observed within the range of 500-4000 cm^{-1}.

2.3 Antifungal efficacy of silver nanoparticles against *A. brassicae*

Tests were performed to analyze the antifungal potential of Ag_2O and Ag NPs on *A. brassicae*

i. *In vitro* antifungal assay

A poisoned food method was conducted to calculate the inhibition percentage of fungus. Three different concentrations (40 ppm, 60 ppm, and 80 ppm) of Ag_2O and Ag NPs were separately prepared on Potato Dextrose Agar (PDA) in triplicate, while plain PDA served as the control. A disc from the peripheral region of a 12 to 14 day old mother culture was transferred to the center of the PDA plates containing different NPs concentrations and then incubated at 22 ± 2°C for fungal colonization. The radial growth of the mycelia was measured at three day intervals until the control reached the edges of the petri plate, using the following formula (Armengol *et al*., 2021).

$$\text{Inhibition per cet} = \frac{C - T}{C} \times 100$$

where:

C = Radial growth (diameter) of mycelia in untreated media

T = Radial growth (diameter) of mycelia in media supplemented with NPs

ii. Morphological analysis

Olympus CX33 optical microscope was used to observe the effect of Ag_2O and Ag NPs on the conidial structure (fruiting bodies) of *A. brassicae*. The conidia were harvested from 12 to 14 day old mother cultures by flooding the PDA plates with autoclaved distilled water, followed by gentle scraping with a sterile loop to dislocate the conidia from the culture. The water was collected and vortexed to separate the conidia from any adhering mycelial fragments. Subsequently, it was filtered through sterile cheesecloth to remove residual mycelial debris and then diluted to prepare a spore suspension containing 10t spores per ml. (Leyronas *et al*., 2012). 40 to 50 conidia from suspension were used to incubate on cavity glass slides containing 60 ppm and 80 ppm concentrations of each NPs (Ag_2O and Ag), while autoclaved distilled water was used as a control. The conidia were then examined for any anomalies at every 12 h over three intervals using a 40X optical microscope (Aremu *et al*., 2003). To examine the effect of silver NPs on fungal growth, SEM analysis was performed on samples collected from PDA plates treated with 80 ppm concentration of both silver NPs. The imprint of Ag_2O_2, Ag samples, and control were collected to observe changes under different resolutions (Ibrahim *et al*., 2020).

iii. Per cent disease intensity (PDI) analysis

The efficacy of silver NPs against Alternaria blight disease was evaluated in *B. juncea* plants. Seeds were sown in pots with three replicates under controlled polyhouse conditions maintained at 25°C and 80% relative humidity. Proper irrigation was provided throughout the growth period. After 45 days, a foliar spray of silver NPs (80 ppm) was applied, while autoclaved distilled water was used as the control. One week after the NPs spray, the plants were deliberately inoculated with *A. brassicae* spores to assess disease progression (Giri *et al*., 2013). Then, the PDI was calculated at different time intervals after the symptoms appeared by using the 0-6 disease rating scale (Table 1), developed by Conn *et al*. (1990); Dhaliwal and Singh (2020).

$$\text{Per cent disease intensity} = \frac{\Sigma(n \times v)}{N \times V} \times 100$$

where:

n = Number of leaves (or plants) in each disease grade

v = Numerical value of each disease grade

N = Total number of leaves (or plants) observed

V = Maximum numerical value on the rating scale

Table 1: Rating scale for Alternaria blight disease

Rating	Area covered with symptoms	Disease reaction
0	0 (No infection)	Immune
1	< 5%	Highly resistant
2	5-10%	Resistant
3	10-20%	Moderately resistant
4	20-30%	Moderately Susceptible
5	30-50%	Susceptible
6	>50%	Highly susceptible

2.4 Statistical analysis

The records used in the study were curated using replicated trials under a completely randomized design (CRD), while the data represented were analysed through ANOVA performed by using OPSTAT software, with statistical significance determined at $p<0.001$.

3. Results

3.1 Physicochemical characterization of silver nanoparticles

3.1.1 UV-Visible spectroscopy analysis

Plasmonic metals are remarkable for absorbing and scattering light efficiently, which can be used to detect the optical characteristics and confirm the formation of NPs through ultraviolet-visible (UV-Vis) spectroscopy technique. The absorption spectrum of metal NPs typically exhibits a bell-shaped curve that peaks at maximum absorption, corresponding to the phenomenon known as localized surface plasmon resonance (SPR). The shape and absorption wavelength of the peak are crucial, as they reveal insight into the particle size distribution and morphological characteristics of NPs. A distinct and intense SPR peak near 400 nm is a reliable indicator of the reduction of silver ions to well-dispersed and stable silver NPs (Christensen *et al*., 2011). However, when this peak shifts to longer (red shift) or smaller wavelengths (blue shift) relative to 400 nm, it typically indicates the presence of larger or smaller sized silver NPs, respectively. The broader or multiple SPR signifies particle aggregation and anisotropic shapes of NPs (Aziz *et al*., 2017). The UV-Visible spectroscopy analysis represents the maximum absorbance value for Ag_2O at 1.25 and Ag at 1.40. The SPR of Ag_2O exhibits a broad range and less defined peak spanning from 330 to 500 nm, indicating large particle size with a wide range of particle distribution (Khatoon and Velidandi, 2024), whereas Ag NPs display a sharp and narrow SPR at 435 nm with absorbance between 340 to 520 nm (Figure 1), indicating uniform, stable and monodisperse particles. The difference between the synthesized NPs could be attributed to faster nucleation during the process of synthesis as well as the type of reducing agent used, temperature and pH of the reaction (Paramelle *et al*., 2014; Nagaraja *et al*., 2022).

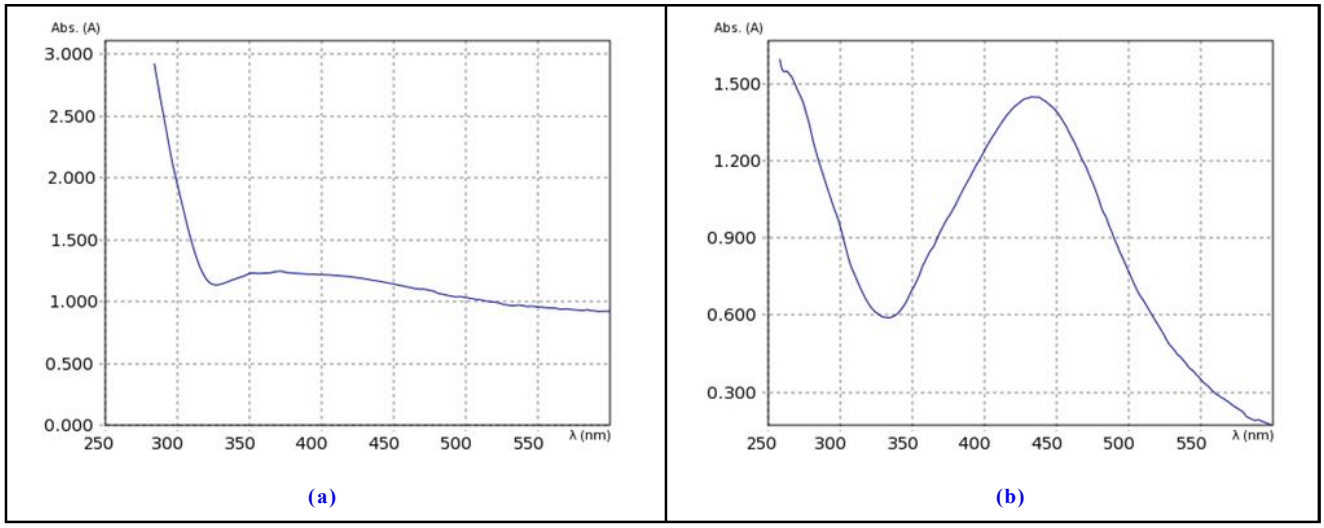

Figure 1: The UV-Visible absorption spectrum of (a) Ag_2O NPs and (b) Ag NPs displaying a characteristic surface plasmon resonance peak.

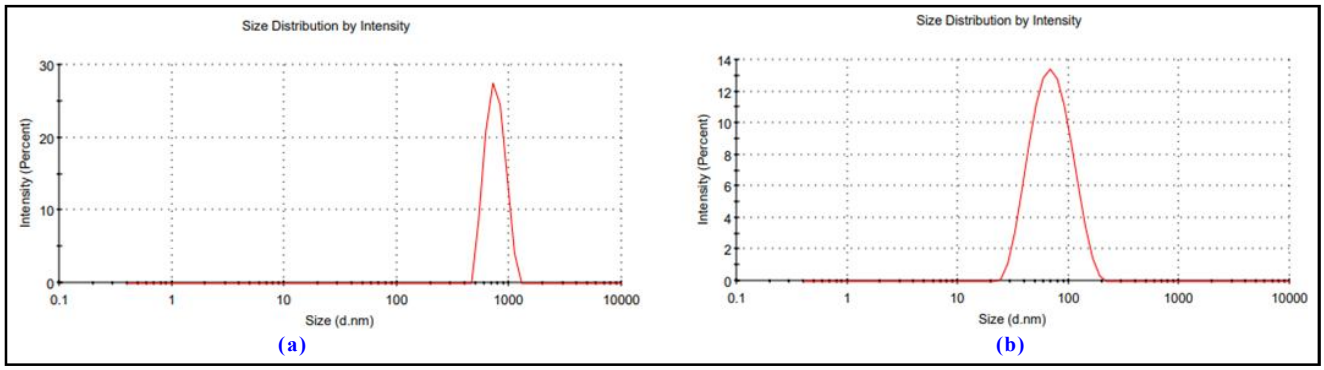

Figure 2: Dynamic light scattering analysis of (a) Ag_2O NPs and (b) Ag NPs displaying the particle size distribution and corresponding polydispersity index.

3.1.2 Dynamic light scattering analysis

Dynamic light scattering (DLS) is well-known as photon correlation spectroscopy, widely used to determine particle size, particle distribution and aggregation. The data acquired from DLS analysis (Figure 2) demonstrate an average size of 747.6 nm for Ag_2O NPs, indicating a significantly larger size. This increased size may be due

to the broader size of the oxide layer, which increases the hydrodynamic diameter of Ag_2O, or may be due to agglomeration (Leong *et al*., 2018). However, the polydispersity index (PDI) of Ag_2O is 0.124, suggesting that the particles are highly monodispersed with uniform size distribution. In contrast, Ag NPs exhibited an average size of 54.79 nm, with a PDI of 0.276, indicating moderately dispersed and less homogeneous in particle size (Chicea *et al*., 2023).

3.1.3 FTIR analysis

FTIR analysis was employed to determine the presence of organic moieties conjugated to the surface of NPs, providing stability during reduction. The FTIR spectrum of Ag_2O and Ag reveals several significant vibrational stretches across 600-4000 cm^{-1} wavelength (Figure 3). For Ag_2O NPs, a broad absorption band was observed between 3757.70 and 2955.92 cm^{-1}, with a prominent peak at 3319 cm^{-1} attributed to O–H stretching vibrations of alcohol and carboxylic groups. Additionally, a smaller peak at 2338.77 cm^{-1} was detected, corresponding to carbon dioxide (C=O) stretching or alkyne (C ≡ C) bending vibrations. A medium peak at 1067 cm^{-1} indicates C–O stretching, suggesting the presence of alcohols or polysaccharides, while the peak at 898.94 cm^{-1} signifies C–H bending vibrations linked with aromatic compounds (Nahar *et al*., 2021). Similarly, the FTIR spectrum of Ag NPs displayed a strong and broad absorption band ranging from 3737.50 to 2953.23 cm^{-1}, with a sharp peak at 3239.68 cm^{-1}, indicating O-H stretching associated with alcohols. A medium peak at 1640.23 cm^{-1} was attributed to C=O stretching or amide (- CO - NH_2) bending vibrations, while a smaller peak at 1067.37 cm^{-1} corresponded to C–N stretching, suggesting the involvement of amines in the reduction of silver ions to Ag NPs. Notably, a strong peak at 671.53 cm^{-1} was observed, which represents C=C bending vibrations, likely associated with alkenes or sulfur-containing groups such as thiols or thioethers (CH, –S–) (Kokila *et al*., 2015; Islam *et al*., 2023) indicating that the organic compounds, including flavonoids, terpenoids, alkaloids, and reducing sugars, were responsible for reducing silver ions to silver NPs while simultaneously capping the surface of NPs to enhance their stability.

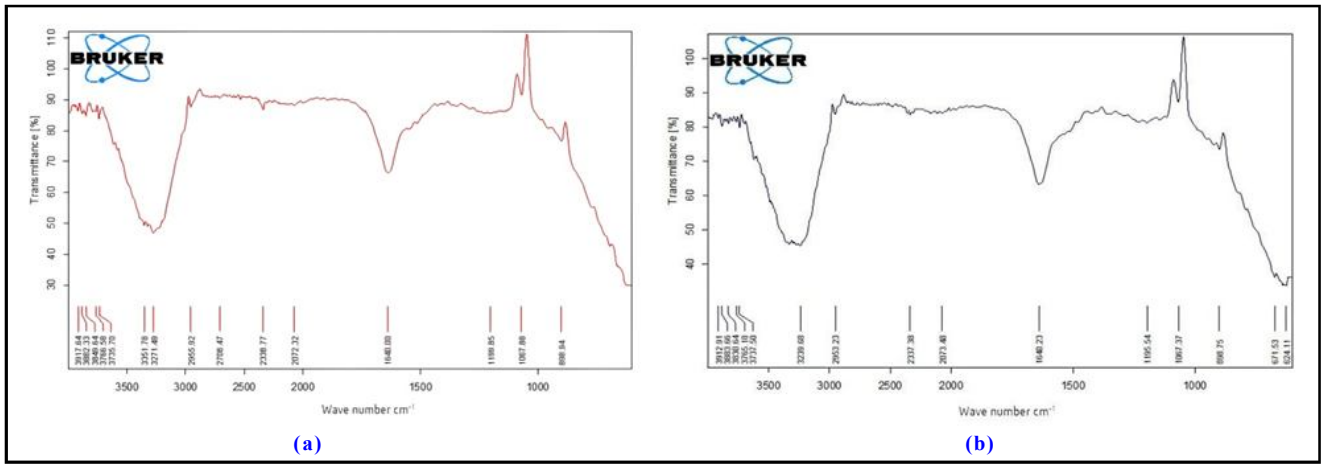

(a) (b)

Figure 3: FTIR analysis of (a) Ag_2O NPs and (b) Ag NPs displaying characteristic absorption peaks corresponding to functional groups involved in NPs formation and stabilization (weak peaks observed in FTIR graph attributed to background noise).

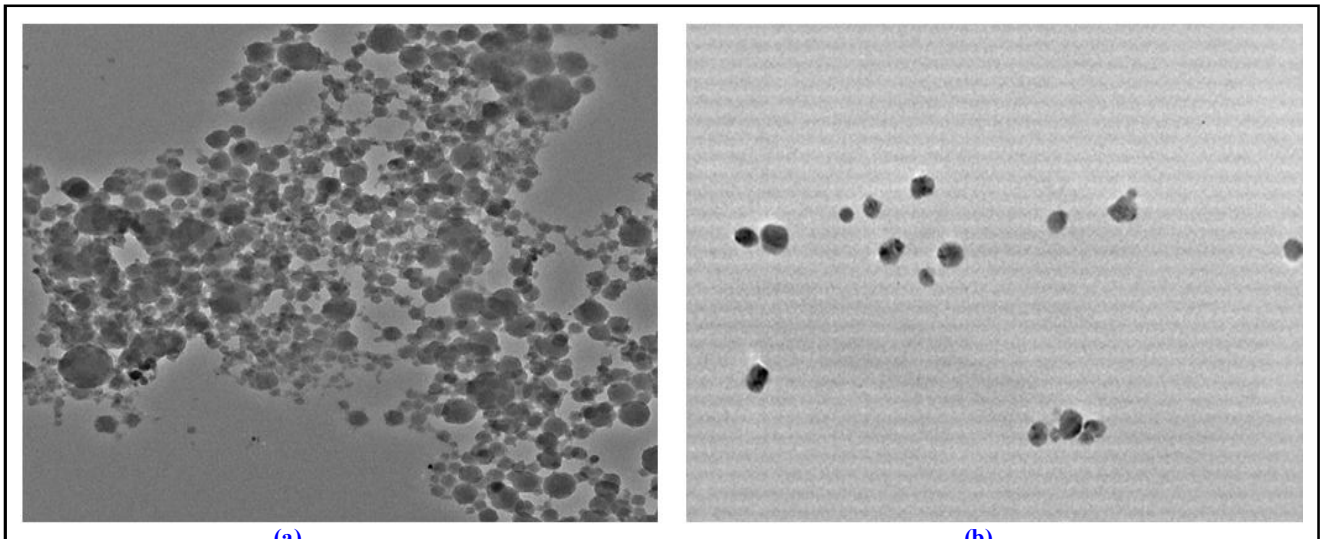

(a) (b)

Figure 4: TEM images of (a) Ag_2O NPs and (b) Ag NPs at 20 µm resolution, displaying morphology, size and particle distribution.

3.1.4 Transmission electron microscopy (TEM) analysis

The surface morphology and distribution of silver NPs were acquired through TEM analysis as represented in Figure 4. The Ag_2O NPs predominantly exhibit spherical to quasi-spherical shape with irregularities in size and non-uniform particle distribution, which occur due to agglomeration or high concentration of particles per volume. Ag NPs appeared mostly spherical to slightly oval and were well dispersed, having a slight difference in particle size, suggesting effective stabilization and synthesis (Martínez *et al*., 2008).

3.2 Antifungal efficacy of silver nanoparticles against *A. brassicae*

3.2.1 *In vitro* antifungal assay

In vitro antifungal assay was evaluated by measuring radial growth of *A. brassicae* and then calculating the per cent inhibition for over four different days across three concentrations (40 ppm, 60 ppm, and 80 ppm) of Ag_2O and Ag NPs. All cultures exhibited cottony and circular patterns. However, significant variations in radial size and colour were observed in both Ag_2O and Ag NPs treated samples (Wen *et al*., 2023). The untreated culture plates displayed a dense green coloration, whereas plates treated with 80 ppm of Ag_2O displayed a moderate green hue and those treated with 80 ppm of Ag appeared off-white (Figure 5) (Shendge *et al*., 2024). These green pigments were considered as melanin and secondary metabolites that play an essential role in facilitating growth under environmental stress (Ramachandra *et al*., 2023). The observed reduction in these pigments suggests that the synthesis of these metabolites and melanin is inhibited, likely due to disruption of fungal metabolic activity as ensured by the reduced fungal growth within treated media (Mishra and Singh, 2015).

The analysis of per cent inhibition across different incubation periods and concentrations revealed that NPs at 80 ppm exhibited the highest antifungal activity against *A. brassicae*, indicating that increasing concentration significantly enhances antifungal efficacy (Osonga *et al*., 2020). Several reports have confirmed that higher NPs concentrations intensify oxidative stress, leading to structural damage in fungal hyphae (Vera-Reyes *et al*., 2022; Li *et al*., 2022). Among all treatments (Table 2), the maximum inhibition across different incubation intervals was observed at 80 ppm Ag NPs, suggesting that smaller particle size amplifies antifungal effects because of improved penetrance (Akpinar *et al*., 2021).

Table 2: Effect of silver NPs at different concentrations on the mycelial growth inhibition per cent of *A. brassicae* at different incubation intervals

Nanoparticles	Concentration	3rd day	6th day	9th day	12th day
Ag_2O	40 ppm	$31.301^{c} \pm 2.03$	$35.038^{c} \pm 0.55$	$31.475^{c} \pm 0.91$	$24.253^{bc} \pm 2.41$
	60 ppm	$32.549^{bc} \pm 1.59$	$35.871^{c} \pm 3.11$	$34.263^{bc} \pm 0.46$	$28.755^{ab} \pm 3.46$
	80 ppm	$39.808^{ab} \pm 4.09$	$58.957^{a} \pm 2.06$	$42.674^{ab} \pm 2.39$	$30.441^{ab} \pm 4$
Ag	40 ppm	$28.949^{c} \pm 2.75$	$34.147^{c} \pm 4.83$	$34.233^{bc} \pm 4.65$	$18.027^{c} \pm 3.08$
	60 ppm	$33.798^{abc} \pm 5.22$	$45.453^{b} \pm 2$	$32.932^{c} \pm 9.32$	$24.253^{bc} \pm 2.41$
	80 ppm	$41.214^{a} \pm 0.73$	$51.257^{b} \pm 2.98$	$46.146^{a} \pm 1.07$	$33.927^{a} \pm 1.7$
LSD		7.551	7.267	8.955	7.323

Values represent mean ± SE. *a, b and c letter represent the statistical grouping of inhibition percentage by using Tukey's HSD multiple comparison test.

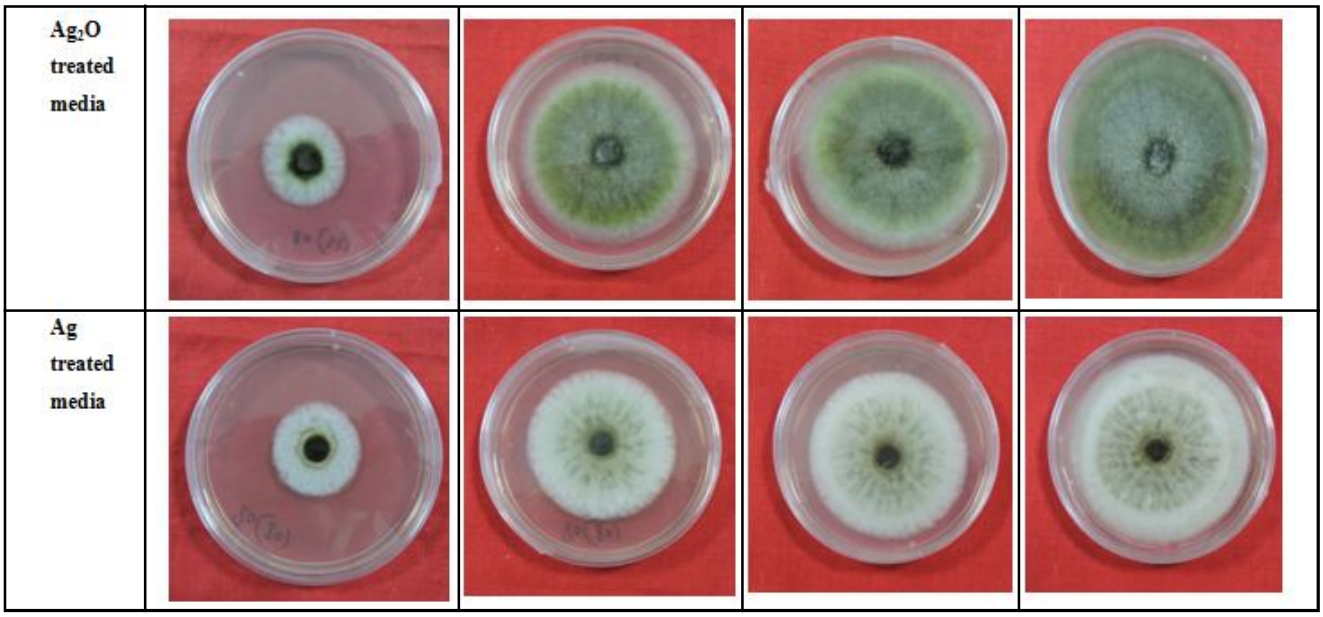

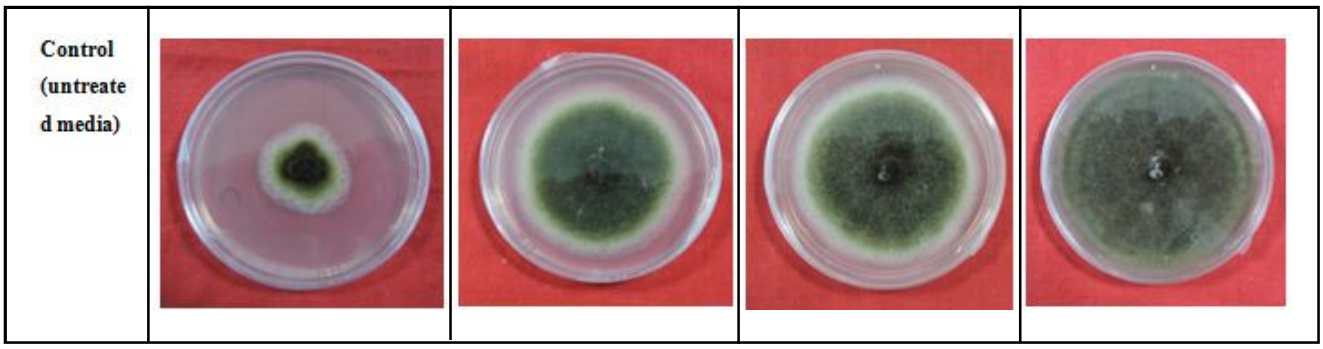

Figure 5: Comparison of *A. brassicae* growth on untreated PDA and PDA supplemented with 80 ppm Ag_2O NPs and Ag NPs.

3.2.2 Morphometric analysis

3.2.2.1 Optical microscopic analysis

During the incubation of *A. brassicae* spores on glass slides, observations were made at three different time intervals (12 h, 24 h, and 36 h). At 12 h, all samples, including the control, had intact spores actively suspended within the cavity slides. By 24 h, control samples began to exhibit early signs of germination, characterized by the formation of bulbous structures at specific regions of the conidia. In contrast, treatments with 60 ppm of Ag and 80 ppm of both Ag_2O and Ag NPs displayed signs of structural damage, including membrane rupture and cytoplasmic leakage, indicating a significant reduction in germination rates at higher NPs concentrations (Ganash *et al*., 2018; Kirti *et al*., 2020). However, spores treated with 60 ppm Ag_2O remained structurally intact, somehow resembling the control. At 36 h, spores in the control, as well as those treated with 60 ppm of both Ag and Ag_2O, developed well-defined germ tubes that extended into septate hyphae emerging from multiple points on the conidia. In contrast, no germination was observed in spores treated with 80 ppm concentrations of either Ag or Ag_2O NPs (Figure 6) (Wagner *et al*., 2016; Gaba *et al*., 2022).

Type of NPs	Concentration of NPs (ppm)	Incubation period		
		6 h	12 h	18 h
Ag_2O	60			
	80			
Ag	60			

Figure 6: Optical microscopic images of *A. brassicae* spores displaying morphological anomalies induced by treatment with 60 ppm and 80 ppm concentrations of Ag_2O and Ag NPs.

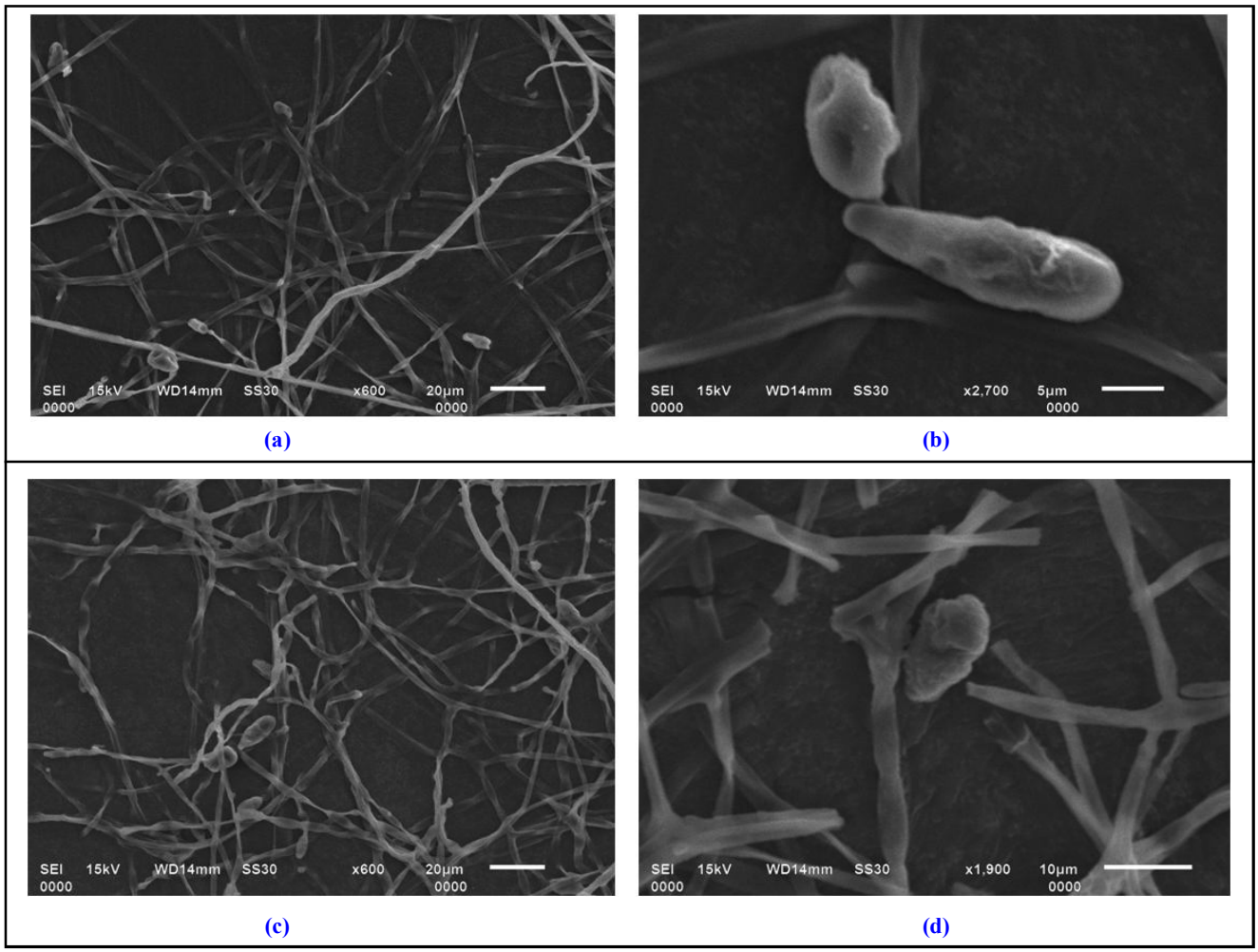

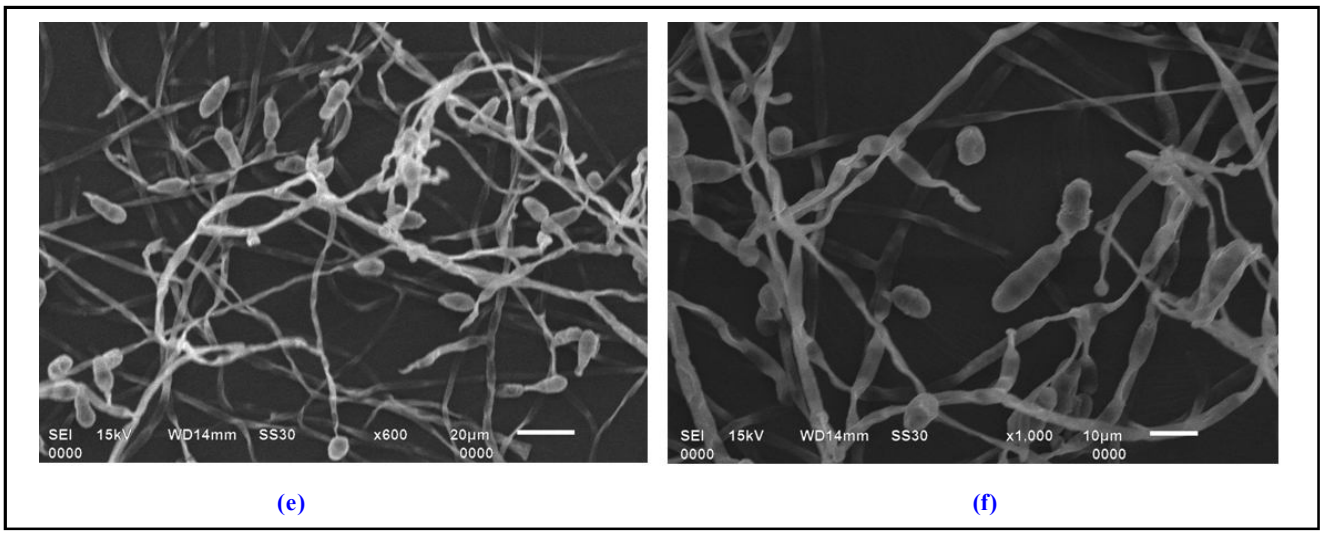

Figure 7: Electron micrographs of *A. brassicae* treated with 80 ppm Ag_2O (a: 20 µm; b: 5 µm), 80 ppm Ag (c: 20 µm; d 10 µm) and control (e: 20 µm; f: 10 µm), illustrating morphological alteration at different resolutions.

3.2.2.2 Scanning electron microscopy (SEM) analysis

The effects of 80 ppm concentration of silver (Ag and Ag_2O) NPs on the mycelial and spore structures of *A. brassicae* were assessed using SEM in Figure 7, at different resolutions. Both 80 ppm of Ag and Ag_2O treated fungus revealed reduced sporulation and significant deformities in the hyphal structure, including crumpled hyphae, shrinkage, depressions and swelling of conidia (Dhiman *et al*., 2022). However, the Ag NPs treated culture exhibits distinct hyphal breakage and less conidia formation compared to Ag_2O, while the untreated sample exhibited abundant sporulation without any structural deformities (Daniel *et al*., 2023).

3.2.3 Disease intensity

The efficacy of Ag_2O and Ag NPs against the fungal pathogen was evaluated at three different time intervals using a standardized grading scale (Table 1), based on lesion formation and foliar damage. Forty-five days after sowing, the plants were treated with 80 ppm concentrations of Ag_2O and Ag NPs in their respective replicates. One week later, the same plants were inoculated with *A. brassicae* spores at a concentration of 10^4 spores/ ml to induce blight disease, maintaining 90% relative humidity to promote sporulation (Timmer *et al*., 1998). By the second day post-inoculation, tiny black-grey spots appeared on both the abaxial and adaxial surfaces of the leaves. These progressively expand into lesions surrounded by yellow halos within 4 to 5 days, particularly more prominent in the control group (Nowicki *et al*., 2022). The number of spots was significantly higher in the control compared to the treated plants. Over time, these spots enlarged into lesions, leading to necrosis and severe leaf damage; additionally, new tiny lesions began to emerge (Figure 8). On final day, plants treated with Ag and Ag_2O NPs exhibited a reduced number of lesions (~18) with 33.33% disease intensity for Ag treated and 39.98 lesions with 21.33% of disease intensity for Ag_2O, indicating slower disease progression and lower severity compared to control group which showed 40 number of lesions with a disease intensity of 58.86% (Table 3) (Summuna *et al*., 2018). The reduction in disease intensity observed in silver NPs treated plants is mainly due to the prior activation of systemic resistance (Masood *et al*., 2024). Silver NPs are considered to serve as potent elicitors, stimulating defense signaling pathways. Moreover, silver NPs also enhance the production of reactive oxygen species (ROS), which not only inhibit pathogen growth but also act as secondary messengers to activate additional plant defense mechanisms that lead to upregulation of pathogenesis-related (PR) genes and defense-associated enzymes (Imada *et al*., 2016). Moreover, Ag NPs treatment significantly increases the expression levels of key antioxidant and phytoalexin pathway genes, promotes the synthesis of phenolics and flavonoids (Ashraf *et al*., 2025).

Table 3: Effect of 80 ppm Ag and 80 ppm Ag_2O NPs on the per cent disease intensity of Alternaria blight in *B. juncea* over different time intervals

Treatments	7th		14th		21st	
	PDI	No. of spots	PDI	No. of spots	PDI	No. of spots
Ag_2O	13.33 ± 1.92	9.33 ± 0.33	29.99 ± 1.92	16 ± 2.08	39.98 ± 1.91	21.33 ± 2.02
Ag	6.663 ± 1.92	9 ± 0.57	26.64 ± 1.92	11.33 ± 1.2	33.33 ± 1.92	18 ± 2.08
Control	32.20 ± 2.93	15.33 ± 1.45	42.18 ± 2.92	22.33 ± 1.45	58.86 ± 5.88	40.33 ± 2.4
C.D.	8.156	3.256	8.136	5.721	13.198	7.681
SE(d)	3.27	1.305	3.262	2.293	5.291	3.079
C.V.	23.014	14.245	12.127	16.965	14.706	14.201

The data presented as the mean of three replicates with corresponding C.D.:critical difference; SE(d): standard error of difference and C.V.: coefficient of variation, with a significance level of $p<0.001$.

Treatments	7 days after pathogen inoculation	14 day after pathogen inoculation	21 days after pathogen inoculation
Ag			
Ag_2O			
Control(water)			

Figure 8: Comparative progression of Alternaria blight disease over 3 days in untreated, 80 ppm Ag NPs and 80 ppm Ag_2O NPs treated *B. juncea* plants.

4. Discussion

This study demonstrates a comparative evaluation of elemental silver (Ag) and silver oxide (Ag_2O) NPs in relation to their physicochemical properties and antifungal efficacy against *A. brassicae*. Characterization through UV-Vis spectroscopy, DLS, FTIR, and TEM revealed significant differences in NPs morphology, size and particle dispersion. The Ag NPs exhibited a sharp surface plasmon resonance at 435 nm, a smaller average size (54.79 nm) and well-dispersed spherical morphology, indicating effective and stable synthesis. In contrast, Ag_2O NPs showed broader absorption, a larger size of 747.6 nm with partial agglomeration; however, the capping moieties in both NPs were found to be quite similar. The differences in NPs, attributed to variations in chemical structure, synthesis routes, reducing agent and growth kinetics, influenced their biological activity (Ashraf *et al*., 2018).

Functionally, both types of NPs showed inhibitory effects on *A. brassicae* growth, with Ag NPs consistently demonstrating superior antifungal activity across *in vitro* and *in vivo* assays. At 80 ppm, Ag NPs achieved the highest per cent inhibition of radial mycelial growth, disrupted spore germination and induced significant morphological deformities, as evidenced by SEM analysis (Kabeerdass *et al*., 2021). Moreover, foliar application of Ag NPs resulted in the maximum reduction in lesion number and disease intensity under greenhouse conditions, affirming their potential in disease suppression due to their smaller size and uniformity in particle size distribution, leading to higher surface reactivity, which enhances penetration into fungal cells (Vera-Reyes *et al*., 2022), whereas Ag_2O NPs were larger, heterogeneous and prone to aggregation (Iravani *et al*., 2014), thus have less effectiveness compared to Ag NPs. The greater efficacy of Ag lies within their structural and chemical properties. Ag NPs are generally more stable than Ag_2O NPs under physiological conditions, allowing for the controlled release of silver ions, whereas Ag_2O dissolves rapidly, leading to depletion of active ions. Additionally, Ag NPs offer greater surface functionality and versatility in synthesis, enabling the incorporation of various ligands, polymers or

biomolecules for targeted delivery and antimicrobial coating (Sati *et al*., 2024; Sergio *et al*., 2025). This approach can reduce the reliance on conventional agrochemicals, which are often associated with cytotoxicity and soil contamination. However, further studies are required to determine the optimal concentration of silver nanoparticles that effectively suppresses Alternaria blight without causing phytotoxic effects on *B. juncea* while maintaining environmental sustainability.

5. Conclusion

This study demonstrates that the two forms of silver NPs (Ag_2O and Ag) exhibit notable variations in their physicochemical characteristics. These variations, along with the NPs concentration, critically influence their antifungal efficacy against *A. brassicae*. The comparative analysis revealed that differences in particle size, morphology and surface moiety significantly affect their inhibitory potential. Furthermore, both *in vivo* and *in vitro* studies confirm that distinct forms as well as different concentrations of silver NPs can exhibit different degrees of antifungal activity, underscoring the importance of NPs composition and surface properties in determining their biological effectiveness and potential application in managing Alternaria blight disease in *B. juncea*.

Acknowledgements

We gratefully acknowledge the Department of Molecular Biology and Genetic Engineering, CBSH, GBPUA&T for their support throughout our research work and Dr. Absar Ahmed, Department of INC, Aligarh Muslim University, for providing the nanoparticles.

Conflict of interest

The authors declare no conflicts of interest relevant to this article.

Authors contribution

1. Sandhya Upadhyay: Manuscript writing, data analysis and result interpretation
2. Anjali Sharma: Manuscript writing
3. S. K. Najrul Islam: Nanoparticle formulation and synthesis
4. Absar Ahmed: Nanoparticle formulation, synthesis and manuscript review
5. Gohar Taj: Conceptualization, data analysis and result interpretation, manuscript review and correction.

List of abbreviations

nm: nano meter

SPR: Surface Plasmon Resonance

DLS: Dynamic Light Scattering

PDI: Per cent Disease Intensity

FTIR: Fourier Transform Infrared Spectroscopy

SEM: Scanning Electron Microscopy

TEM: Transmission Electron Microscopy

LSD: Least Significant Difference

References

Abdallah, I.; Yehia, R. and Kandil, M.A.H. (2020). Biofumigation potential of Indian mustard (*Brassica juncea*) to manage Rhizoctonia solani. Egypt. J. Biol. Pest Control, **30**(1):99.

Akpinar, I.; Unal, M. and Sar, T. (2021). Potential antifungal effects of silver nanoparticles (AgNPs) of different sizes against phytopathogenic *Fusarium oxysporum* f. sp. radicis-lycopersici (FORL) strains. SN Appl. Sci., **3**(4):506.

Aremu, E.A.; Furumai, T.; Igarashi, Y.; Sato, Y., Akamatsu, H.; Kodama, M. and Otani, H. (2003). Specific inhibition of spore germination of *Alternaria brassicicola* by fistupyrone from *Streptomyces* sp. TP-A0569. J. Gen. Plant pathol., **69**:211-217.

Armengol, E.S.; Harmanci, M. and Laffleur, F. (2021). Current strategies to determine antifungal and antimicrobial activity of natural compounds. Microbiol. Res., **252**:126867.

Ashraf, H.; Anjum, T.; Ahmad, I.S.; Ahmed, R.; Aftab, Z.E.H. and Rizwana, H. (2025). Phytofabricated silver nanoparticles unlock new potential in tomato plants by combating wilt infection and enhancing plant growth. Sci. Rep., **15**(1):10527.

Ashraf, M.A.; Peng, W.; Zare, Y. and Rhee, K.Y. (2018). Effects of size and aggregation/agglomeration of nanoparticles on the interfacial/interphase properties and tensile strength of polymer nanocomposites. Nanoscale Res. Let., **13**(1):214.

Aziz, S.B.; Abdullah, O.G.; Saber, D.R.; Rasheed, M.A. and Ahmed, H.M. (2017). Investigation of metallic silver nanoparticles through UV-Vis and optical micrograph techniques. Int. J. Electrochem. Sci., **12**(1):363-373.

Bhunjun, C.S.; Phillips, A.J.; Jayawardena, R.S.; Promputtha, I. and Hyde, K.D. (2021). Importance of molecular data to identify fungal plant pathogens and guidelines for pathogenicity testing based on Koch's postulates. Pathogens, **10**(9):1096.

Chicea, D.; Nicolae-Maranciuc, A.; Doroshkevich, A.S.; Chicea, L.M. and Ozkendir, O.M. (2023). Comparative synthesis of silver nanoparticles: Evaluation of chemical reduction procedures, AFM and DLS size analysis. Mater., **16**(15):5244.

Christensen, L.; Vivekanandhan, S.; Misra, M. and Kumar Mohanty, A. (2011). Biosynthesis of silver nanoparticles using *Murraya koenigii* (curry leaf): an investigation on the effect of broth concentration in reduction mechanism and particle size. Adv. Mater. Lett., **2**(6):429-434.

Conn, K.L.; Tewari, J.P. and Awasthi, R.P. (1990). A disease assessment key for Alternaria blackspot in rapeseed and mustard. Can. Plant Dis. Surv., **70**(1):19-22.

Daniel, A.I.; Al-Hashimi, A.; Keyster, M. and Klein, A. (2023). Phyto-synthesis and characterization of silver nanoparticles using box-behnken design and its anti-alternaria activity. Clean Technol., **5**(4):1381-1401.

Dhaliwal, R.S. and Singh, B. (2020). Effect of weather parameters and date of sowing on intensity of Alternaria blight of rapeseed mustard. Indian Phytopathol., **73**(1):89-95.

Dhiman, S.; Varma, A.; Prasad, R. and Goel, A. (2022). Mechanistic insight of the antifungal potential of green synthesized zinc oxide nanoparticles against *Alternaria brassicae*. J. Nanomater., **2022**(1):7138843.

Ficerman, W.; Wiœniewski, M. and Roszek, K. (2022). Interactions of nanomaterials with cell signalling systems-focus on purines-mediated pathways. Colloids Surf. B Biointerfaces, **220**:112919.

Gaba, S.; Varma, A.; Prasad, R. and Goel, A. (2022). Exploring the impact of bioformulated copper oxide nanoparticles on cytomorphology of *Alternaria brassicicola*. Curr. Microbiol., **79**(8):244.

Ganash, M.; Abdel Ghany, T.M. and Omar, A.M. (2018). Morphological and biomolecules dynamics of phytopathogenic fungi under stress of silver nanoparticles. Bio. Nano. Sci., **8**(2):566-573.

Giri, P.; Taj, G. and Kumar, A. (2013). Comparison of artificial inoculation methods for studying pathogenesis of *Alternaria brassicae* (Berk.) Sacc on *Brassica juncea* (L.) Czern (Indian mustard). Afr. J. Biotechnol., **12**(18).

Hashim, M.; Al-Attar, A.M. and Zeid, I.M.A. (2023). Toxicological effects of carbendazim: a review. Acta Sci. Med. Sci. (ISSN: 2582-0931), **7**(4).

Ibrahim, E.; Luo, J.; Ahmed, T.; Wu, W.; Yan, C. and Li, B. (2020). Biosynthesis of silver nanoparticles using onion endophytic bacterium and its antifungal activity against rice pathogen *Magnaporthe oryzae*. J. Fungi, **6**(4):294.

Imada, K.; Sakai, S.; Kajihara, H.; Tanaka, S. and Ito, S. (2016). Magnesium oxide nanoparticles induce systemic resistance in tomato against bacterial wilt disease. Plant Pathol., **65**(4):551-560.

Iravani, S.; Korbekandi, H.; Mirmohammadi, S.V. and Zolfaghari, B. (2014). Synthesis of silver nanoparticles: Chemical, physical and biological methods. Res. Pharm. Sci., **9**(6):385-406.

Islam, M.J.; Khatun, N.; Bhuiyan, R.H.; Sultana, S.; Shaikh, M.A.A.; Bitu, M.N.A.; Chowdhury, F. and Islam, S. (2023). *Psidium guajava* leaf extract mediated green synthesis of silver nanoparticles and its application in antibacterial coatings. RSC Adv., **13**(28):19164-19172.

Kabeerdass, N.; Al Otaibi, A.; Rajendran, M.; Manikandan, A.; Kashmery, H.A.; Rahman, M.M.; Madhu, P.; Khan, A.; Asiri, A.M. and Mathanmohun, M. (2021). Bacillus-mediated silver nanoparticle synthesis and its antagonistic activity against bacterial and fungal pathogens. Antibiotics, **10**(11):1334.

Kale, S.K.; Parishwad, G.V. and Patil, A.S.H.A.S. (2021). Emerging agriculture applications of silver nanoparticles. ES Food Agrofor., **3**:17-22.

Khatoon, U.T. and Velidandi, A. (2024). Silver oxide nanoparticles: synthesis via chemical reduction, characterization, antimicrobial, and cytotoxicity studies. Inorg. Chem. Commun., **159**:111690.

Kokila, T.; Ramesh, P.S. and Geetha, D.J.A.N. (2015). Biosynthesis of silver nanoparticles from Cavendish banana peel extract and its antibacterial and free radical scavenging assay: A novel biological approach. Appl. Nanosci., **5**:911-920.

Kriti, A.; Ghatak, A. and Mandal, N. (2020). Inhibitory potential assessment of silver nanoparticle on phytopathogenic spores and mycelial growth of *Bipolaris sorokiniana* and *Alternaria brassicicola*. Int. J. Curr. Microbiol. Appl. Sci., **9**(3):692-699.

Kumar, A.; Kumar, R.; Kumar, S.; Nandan, D.; Chand, G. and Kolte, S.J. (2016). Alternaria blight of oilseed brassicas: A review on management strategies through conventional, non-conventional and biotechnological approaches. J. Appl. Nat. Sci., **8**(2):1110

Leong, S.S.; Ng, W.M.; Lim, J. and Yeap, S.P. (2018). Dynamic light scattering: effective sizing technique for characterization of magnetic nanoparticles. Handb. Mater. Charact. (77-111). Cham: Springer International Publishing.

Leyronas, C.; Duffaud, M. and Nicot, P.C. (2012). Compared efficiency of the isolation methods for *Botrytis cinerea*. Mycology, **3**(4):221-225

Li, L.; Pan, H.; Deng, L.; Qian, G.; Wang, Z.; Li, W. and Zhong, C. (2022). The antifungal activity and mechanism of silver nanoparticles against four pathogens causing kiwifruit post-harvest rot. Front. Microbiol., **13**:988633.

Martínez-Castañón, G.A.; Nino-Martinez, N.; Martinez-Gutierrez, F.; Martínez-Mendoza, J.R. and Ruiz, F. (2008). Synthesis and antibacterial activity of silver nanoparticles with different sizes. J. Nanopart. Res., **10**:1343-1348.

Masood, H.A.; Qi, Y., Zahid; M.K., Li, Z.; Ahmad, S.; Lv, J.M.; Shahid, M.S.; Ali, H.E.; Ondrasek, G. and Qi, X. (2024). Recent advances in nano-enabled immunomodulation for enhancing plant resilience against phyto-pathogens. Front. Plant Sci., **15**:1445786.

Meena, P.D.; Rani, A.; Meena, R.; Sharma, P.; Gupta, R. and Chowdappa, P. (2012). Aggressiveness, diversity and distribution of *Alternaria brassicae* isolates infecting oilseed Brassica in India. Afr. J. Microbiol. Res., **6**(24):5249-5258.

Mishra, S. and Singh, H.B. (2015). Silver nanoparticles mediated altered gene expression of melanin biosynthesis genes in *Bipolaris sorokiniana*. Microbiol. Res., **172**:16-18.

Nagaraja, S.; Ahmed, S.S.; DR, B.; Goudanavar, P.; Fattepur, S.; Meravanige, G.; Shariff, A.; Shiroorkar, P.N.; Habeebuddin, M. and Telsang, M. (2022). Green synthesis and characterization of silver nanoparticles of *Psidium guajava* leaf extract and evaluation for its antidiabetic activity. Molecules, **27**(14):4336.

Nahar, K.; Rahaman, M.; Khan, G.M.A.; Islam, M. and Al-Reza, S.M. (2021). Green synthesis of silver nanoparticles from *Citrus sinensis* peel extract and its antibacterial potential. Asian Journal of Green Chemistry, **5**(1):135-150.

Nowicki, M.; Nowakowska, M.; Niezgoda, A. and Kozik, E. (2012). Alter naria black spot of crucifers: symptoms, importance of disease, and perspectives of resistance breeding. Veg. Crops Res. Bull., **76**:5.

Osonga, F.J.; Akgul, A.; Yazgan, I.; Akgul, A.; Eshun, G.B.; Sakhaee, L. and Sadik, O.A. (2020). Size and shape-dependent antimicrobial activities of silver and gold nanoparticles: A model study as potential fungicides. Molecules, **25**(11):2682.

Paramelle, D.; Sadovoy, A.; Gorelik, S.; Free, P.; Hobley, J. and Fernig, D.G. (2014). A rapid method to estimate the concentration of citrate capped silver nanoparticles from UV-visible light spectra. Analyst, **139**(19):4855-4861.

Pirozzi, A.V.A.; Stellavato, A.; La Gatta, A.; Lamberti, M. and Schiraldi, C. (2016). Mancozeb, a fungicide routinely used in agriculture, worsens nonalcoholic fatty liver disease in the human HepG2 cell model. Toxicol. Lett., **249**:1-4.

Ramachandra, S.K.; Kaushik, S.; Austin, H.; Kumar, R. and Parthiban, M. (2023). The role of melanin in plant pathogenic fungi: Insights into structure, biosynthesis, and function. Plant Biol. Crop Res., **6**:1090.

Regar, R.; Meena, A.K.; Goyal, S.K.; Sharma, P.K. and Meena, D.K. alternaria blight disease of indian mustard and its important management practices. an eco-friendly practices disease management:51

Sati, A.; Ranade, T. N.; Mali, S. N.; Ahmad Yasin, H. K., and Pratap, A. (2025). Silver nanoparticles (AgNPs): Comprehensive insights into bio/synthesis, key influencing factors, multifaceted applications, and toxicity% a 2024 update. ACS Omega, **10**(8):7549-7582.

Sergio, L.; Raluca, V.; Lavinia, L.; Elena-Alina, M.; Delia, M., Lucian, B. T. and Francisc, P. (2025). Synthesis of Ag_2O/Ag nanoparticles using puerarin: Characterization, cytotoxicity, In: Ovo Safety Profile, Antioxidant, and Antimicrobial Potential Against Nosocomial Pathogens. J. Funct. Biomater., **16**(7):258.

Sharma, A.; Kumar, V.; Kanwar, M.K.; Thukral, A.K. and Bhardwaj, R. (2017). Phytochemical profiling of the leaves of *Brassica juncea* L. using GC-MS. Int. Food Res. J., **24**(2):547.

Shendge, V.S.; Magar, S.J. and Somwanshi, S.D. (2024). *In vitro* Antifungal Efficacy of Silver Nanoparticles against *Fusarium oxysporum* f. sp. Lycopersici in Tomato. Microbiol. Res. J. Int., **34**(3):1-9.

Strandberg, J.O. (1987). Isolation, storage, and inoculum production methods for *Alternaria dauci*. Phytopathology, **77**(7):1008-1012.

Summuna, B.; Gupta, S. and Sheikh, P.A. (2018). Assessing the disease severity of Alternaria blight of rapeseed-mustard in jammu province of J&K and screening of germplasm against the disease. Int. J. Curr. Microbiol. Appl. Sci., **7**(11):1299-1310

Thakur, A. K.; Parmar, N.; Singh, K. H., and Nanjundan, J. (2020). Current achievements and future prospects of genetic engineering in Indian mustard (*Brassica juncea* L. Czern & Coss.). Planta, **252**(4): 56.

Timmer, L.W.; Solel, Z.; Gottwald, T.R.; Ibanez, A.M. and Zitko, S.E. (1998). Environmental factors affecting production, release, and field populations of conidia of *Alternaria alternata*, the cause of brown spot of citrus. Phytopathology, **88**(11):1218-1223.

Vera-Reyes, I.; Altamirano-Hernández, J.; Reyes-De la Cruz, H.; Granados-Echegoyen, C.A.; Loera-Alvarado, G.; López-López, A. Garcia-Cerda, L.A. and Loera-Alvarado, E. (2022). Inhibition of phytopathogenic and beneficial fungi applying silver nanoparti 3 cles *in vitro*. Molecules, **27**(23):8147.

Verma, S.; Dubey, N.; Singh, K.H.; Parmar, N.; Singh, L.; Sharma, D.; Rana, D.; Thakur, K.; Vaidya, D. and Thakur, A.K. (2023). Utilization of crop wild relatives for biotic and abiotic stress management in Indian mustard [*Brassica juncea* (L.) Czern. & Coss.]. Front. Plant Sci., **14**:1277922.

Wagner, G.; Korenkov, V.; Judy, J.D. and Bertsch, P.M. (2016). Nanoparticles composed of Zn and ZnO inhibit *Peronospora tabacina* spore germination *in vitro* and *P. tabacina* infectivity on tobacco leaves. Nanomaterials, **6**(3):50.

Wen, H.; Shi, H.; Jiang, N.; Qiu, J.; Lin, F. and Kou, Y. (2023). Antifungal mechanisms of silver nanoparticles on mycotoxin producing rice false smut fungus. Iscience, **26**(1).

Zhang, K.; Yuan-Ying, S. and Cai, L. (2013). An optimized protocol of single spore isolation for fungi. Cryptogam. Mycol., **34**(4):349-356.

Citation **Sandhya Upadhyay, Anjali Sharma, S. K. Najrul Islam, Absar Ahmad and Gohar Taj (2025). Analysis of physicochemical characteristic and antifungal potential of silver nanoparticles against Alternaria blight pathogenesis in *Brassica juncea*. Ann. Phytomed., 14(2):668-679. http://dx.doi.org/10.54085/ap.2025.14.2.67.**